Atomic Hydrogen Reactions with P_b Centers at the (100) Si/SiO_2 Interface

J. H. Stathis and E. Cartier
IBM Research Division, T.J. Watson Research Center, Yorktown Heights, New York 10598
(Received 10 November 1993)

We have investigated the reaction of atomic hydrogen with defects at the (100) Si/SiO_2 interface. Similar to previous results on the (111) interface, we find that the two paramagnetic defects at the (100) interface, P_{b0} and P_{b1}, are either passivated or produced by atomic hydrogen, depending on the starting density. However, the two defects possess quantitative differences in behavior. The P_{b0} center can be produced more readily than P_{b1} and it is also much harder to passivate by atomic hydrogen. These differences between P_{b0} and P_{b1} help to explain previous observations of P_{b0} center generation by radiation and by electrical stress.

PACS numbers: 68.35.Dv, 82.30.Cf, 85.30.Tv

The reaction of atomic hydrogen (H^0) with defects at the Si/SiO_2 interface is a subject of considerable scientific as well as technological interest. It is now commonly accepted that atomic hydrogen plays a crucial role in the chemistry of Si/SiO_2 defects. Convincing evidence for the involvement of both atomic hydrogen and protons in the generation of Si/SiO_2 interface defects by radiation has been reviewed by Griscom [1]. Hydrogen also appears to be the dominant agent of interface degradation and eventual oxide breakdown caused by electrical stress [2,3].

The chemical reaction that is usually deemed responsible for hydrogen-induced interface state creation is

$$\text{Si-H} + \text{H}^0 \rightarrow \text{Si-} + \text{H}_2 . \quad (1)$$

Here, Si- represents a dangling bond. Note that in reaction (1) the atomic hydrogen on the left hand side may also be a proton; in that case an electron is supplied from the silicon substrate. Brower and Myers [4] have provided an argument that this reaction, as well as the passivation reaction

$$\text{Si-} + \text{H}^0 \rightarrow \text{Si-H} , \quad (2)$$

should be exothermic with at most a very small energy barrier. In spite of a plethora of circumstantial evidence pointing to such reactions, it has only recently been directly demonstrated [5] that atomic hydrogen actually produces and passivates Si dangling bonds at the Si/SiO_2 interface in this way.

Strictly speaking, reactions (1) and (2) have only been shown [5] to apply to the (111) Si/SiO_2 interface. At this interface there is a single variety of silicon dangling bond defect, the P_b center [6]. Because of its relative simplicity, the majority of fundamental research on defects at the Si/SiO_2 interface has concerned the (111) interface and our knowledge of the structure of the P_b center at this interface is by now quite detailed [7–13].

However, the (100) interface is the preferred one for semiconductor integrated circuits, so it is crucial to understand the chemistry of defects at this specific interface. Here the defect structure is more complex and our understanding is less complete. Two seemingly related defects called P_{b0} and P_{b1} are observed. For the sample oriented with the [100] direction along the magnetic field, these have g values of 2.0060 and 2.0032, respectively [14]. The precise structure of these two defects, and their relation to the single variety of P_b defect observed at the (111) interface, is still a matter of some controversy [15,16], and it has been shown [17] that the kinetics of hydrogen annealing of electrically active interface states is different for (100) and (111). Nevertheless, since both defects on (100) are considered to be silicon dangling bonds, naively one would expect their response to atomic hydrogen to be identical.

In this Letter we prove that this is not the case. We investigate the reaction of P_{b0}^{100} and P_{b1}^{100} centers [18] at the (100) interface with atomic hydrogen from a remote plasma, and find that they show marked differences in their chemical behavior. These results help to clarify previous electron paramagnetic resonance (EPR) studies of electrical stress and radiation effects on (100) oriented samples, and lead us to point out significant difficulties in attempting to generalize fundamental studies of the simpler (111) interface to the technologically important (100) interface.

High resistivity ($> 100\ \Omega\,\text{cm}$) silicon wafers of (111) and (100) orientation, polished on both sides, were oxidized in a standard open tube furnace in dry oxygen at 900 °C. Oxide thicknesses were 9.75 nm for the (111) wafers and 67.5 nm for the (100) wafers. The steady-state dangling bond densities which are discussed in this paper are independent of oxide thickness. Some of the wafers were annealed in vacuum ($\leq 10^{-7}$ torr) for 120 min at 700–800 °C in order to produce P_b centers by driving off hydrogen [4] [the reverse of reaction (2)]. The apparatus for atomic hydrogen exposure has been described previously [5]. All exposures were done at room temperature. Standard room-temperature EPR measurements (~9.6 GHz) were performed. Total spin densities were obtained by double numerical integration of the experimental first-derivative spectra and comparison with a calibrated ruby standard. Individual densities of P_{b0}^{100} and P_{b1}^{100} centers were extracted by fitting to Voigt line

0031-9007/94/72(17)/2745(4)$06.00

shapes. All spectra for the (100) orientation were fit simultaneously by a single set of line-shape parameters and g values for P_{b0}^{100} and P_{b1}^{100}, allowing only the amplitudes of the two lines to vary independently in each spectrum. This procedure minimizes error arising from baseline variations, which otherwise might lead to apparent variations in the linewidths. The optimum fit corresponded, for P_{b0}^{100}, to a Guassian of peak-to-peak first derivative width 3.84 ± 0.04 G and, for P_{b1}^{100}, a Voigt line with Gaussian and Lorentzian component widths of 3.2 ± 0.12 and 0.13 ± 0.06 G, respectively. The relative accuracy of paramagnetic defect densities quoted in this paper is $\pm 10\%$. The absolute accuracy is approximately $\pm 50\%$. A modulation amplitude of 2.2 G was used for the (111) oriented samples for optimum signal-to-noise ratio, while 1 G was used for the (100) oriented samples to resolve the P_{b0}^{100} and P_{b1}^{100} resonances.

The behavior of P_b-type defects at (111) and (100) interfaces when exposed to H^0 is illustrated in the EPR spectra of Figs. 1 and 2. The results for the (111) interface have been described previously [5]: P_b^{111} centers are generated by H^0 in a sample with initial low P_b^{111} density and reduced (passivated) to about the same level if the starting P_b^{111} density is high. Thus, both depassivation and passivation occur according to reactions (1) and (2) and their steady-state balance determines the final P_b^{111} density, $[P_b^{111}]$. In the data illustrated in Fig. 1 the top curve corresponds to $[P_b^{111}] = 2.4 \times 10^{12}$ cm^{-2} and the middle two curves (after H^0 exposure) correspond to 4.5×10^{11} and 3.0×10^{11} cm^{-2}, respectively. As can be seen in Fig. 2, the interaction of the two defects at the (100) interface with atomic hydrogen is quite different. Starting with a low total P_b density results predominantly in the generation of P_{b0}^{100} centers. In contrast, starting

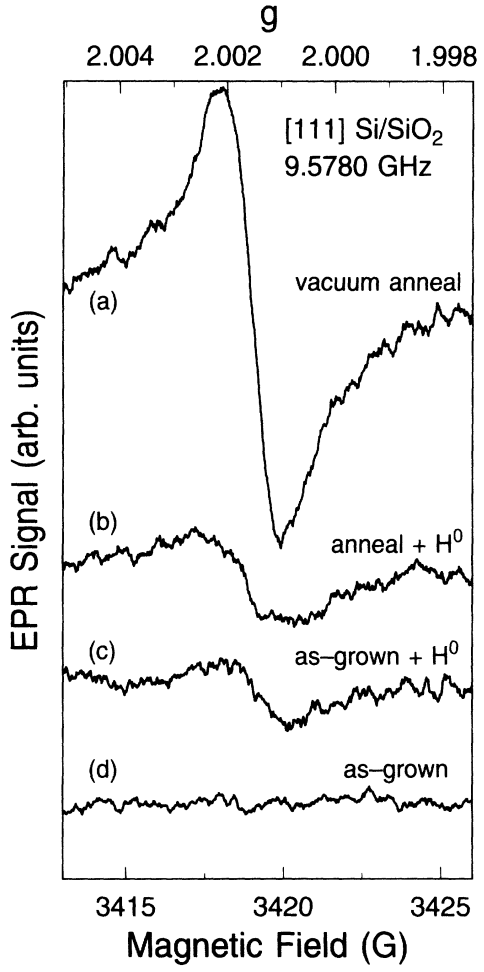

FIG. 1. EPR spectra showing the effect of H^0 on P_b centers at the (111) interface. P_b centers are either generated or passivated, depending on their initial density. (a) Vacuum annealed at 700 °C for 120 min; (b) same as (a) after atomic hydrogen exposure; (c) same as (d) after atomic hydrogen exposure; and (d) as-grown. The magnetic field is parallel to the [111] axis.

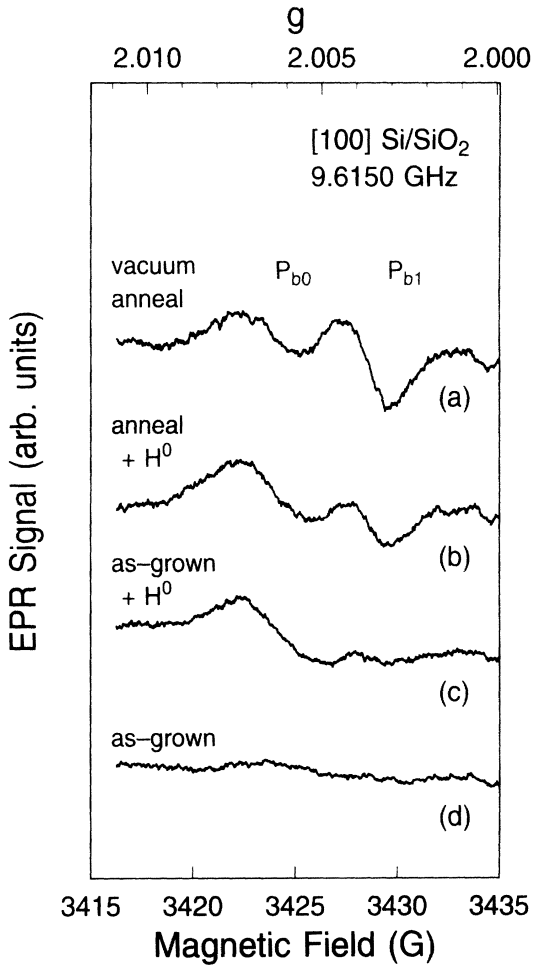

FIG. 2. Effect of H^0 on P_b centers at the (100) interface. (a) Vacuum annealed at 800 °C for 120 min; (b) same as (a) after atomic hydrogen exposure; (c) same as (d) after atomic hydrogen exposure; and (d) as-grown. The magnetic field is parallel to the [100] axis.

with high (and approximately equal) numbers of P_{b0}^{100} and P_{b1}^{100}, we see that only P_{b1}^{100} is markedly passivated by H^0.

The top curve in Fig. 2 is of a sample which has been vacuum annealed, resulting in a high density of P_b centers with $[P_{b0}^{100}]=5.0\times10^{11}$ and $[P_{b1}^{100}]=4.2\times10^{11}$ cm^{-2}. After H^0 exposure, $[P_{b0}^{100}]$ has changed negligibly whereas $[P_{b1}^{100}]$ has decreased to $\sim3.5\times10^{11}$ cm^{-2}. The slight increase in P_{b0} seen in Fig. 2(b) was not seen in all samples. The bottom curve in Fig. 2 is as-grown in a standard tube furnace. A small signal, corresponding to about 1.2×10^{11} spins/cm^2 is seen at $g=2.0048\pm0.0004$, probably arising from residual substrate damage remaining after etching the scribed edges of the sample. After exposure to H^0, we find $[P_{b0}^{100}]=6.0\times10^{11}$ and $[P_{b1}^{100}]=1.2\times10^{11}$ cm^{-2}. Thus, P_{b0}^{100} has been generated to a density equivalent (within experimental uncertainty) to that seen in the vacuum annealed sample, whereas P_{b1}^{100} is created in much smaller quantity.

A concern when studying P_b centers at the (100) interface is interference by the signal from the damaged edges of the sample, which occurs near the P_{b0}^{100} resonance when the magnetic field is oriented parallel to [100]. To reduce this signal, the sample edges were etched. In addition, we performed careful multiline fitting of the spectra. While sometimes improved fits were obtained by adding a third Gaussian component like the line observed in the as-grown sample (bottom curve in Fig. 2), the ratio $[P_{b0}]/[P_{b1}]$ was little changed and no systematic trends in the amplitude of such a third component could be discerned. As a final test we measured the angular dependence of the EPR spectra. It was found to be consistent with the known [6] g matrices of P_{b0}^{100} and P_{b1}^{100}. The edge signal therefore can be neglected.

From the data in Figs. 1 and 2, it can be seen that the P_b^{111} and P_{b1}^{100} reactions show a comparable pattern. For both of these defects, H^0 exposure results in a defect density less than the maximum density $[P_b]^{max}$ obtainable by vacuum annealing. These results confirm earlier findings [16], where it has been observed that P_b^{111} and P_{b1}^{100} are similar to each other and different from P_{b0}^{100} in their response to variations in the oxide growth conditions. The P_{b0}^{100} center is unique in that the steady-state $[P_{b0}^{100}]$ during H^0 exposure is within experimental accuracy found to be equal to $[P_{b0}^{100}]^{max}$. We have previously argued [5] that the steady-state density reflects the difference in the magnitude of the rates of reactions (1) and (2). The steady-state P_b density is

$$\frac{[P_b]}{[P_b]^{max}}=\frac{\sigma_1}{\sigma_1+\sigma_2}, \tag{3}$$

where σ_1 and σ_2 are, respectively, the cross sections for generation and passivation of dangling bonds by atomic hydrogen. According to the experiments shown in Figs. 1 and 2, for P_b^{111} the cross section ratio is $\sigma_2/\sigma_1=5.7\pm1.7$ while for P_{b0}^{100} it is $\sigma_2/\sigma_1\leq0.1$. The steady-state density for P_{b1}^{100} is less well defined. The final density differs by a factor of 3 depending on whether we start from the as-grown or vacuum anneal state. Further H^0 exposure did not alter this situation. The origin of the discrepancy is not clear at present; for P_{b1}^{100} the thermal history of the sample may be important. For example, the vacuum anneal may irreversibly affect the interface structure. This has been generally assumed [13,19] not to be the case in studies of P_b^{111}. Under the assumption that reactions (1) and (2) are valid we find $0.2\leq\sigma_2/\sigma_1\leq2.5$ for P_{b1}^{100}. Thus, none of these defects are identical quantitatively, even though the qualitative behaviors of P_{b1}^{100} and P_b^{111} are similar.

Our atomic hydrogen experiments are directly related to the microscopic degradation physics in electronic devices, because both radiation and hot-electron stress are known to liberate atomic hydrogen from within the oxide (or from the oxide/gate-metal interface) [1,20]. Based on this premise, our observation that the P_{b0}^{100} center is more efficiently generated by atomic hydrogen nicely explains the observation by several groups [21–23] that only P_{b0}^{100} is generated by radiation or electrical stress in (100) oriented devices. Kim and Lenahan [21] observed that γ irradiation of a thermal oxide produced mostly P_{b0}^{100}, with only a small amount of P_{b1}^{100}; their spectrum closely resembles that seen after H^0 exposure in Fig. 2. Using spin-dependent recombination, others [22,23] have detected a spectrum corresponding to P_{b0}^{100} in electrically stressed transistors. The spectrum reported by these authors exhibits an asymmetry, being broader on the high-field side. The results in Fig. 2 suggest that this asymmetry may be explained by a small unresolved P_{b1}^{100} component.

These results have significant implications for the interpretation of other electrical data as well. We previously showed [5] that for the (111) interface the P_b^{111} center can account for only a fraction of the H^0-generated interface states. Preliminary results indicate that paramagnetic defects likewise do not account for all of the electrically active defects at the (100) interface. The spin-dependent recombination results [23] on electrically stressed transistors support this supposition. These experiments show that P_{b0}^{100} is produced by hot electrons, but it cannot account for all of the interface states. Still, P_{b0}^{100} may play a more significant role than does P_b^{111}, because the H^0-generated P_{b0}^{100} density can be larger than that of P_b^{111} while, simultaneously, interface state densities are typically a factor of 2 lower on (100) compared to (111). However, to the extent that *any* of the electrically active radiation- or stress-induced interface defects at the (100) Si/SiO_2 interface are P_b-type defects, the results presented in this Letter demonstrate that such defect is most probably the P_{b0}^{100} center, not P_{b1}^{100}. Particular care is advised when attempting microscopic interpretation of electrical (nonspectroscopic) data in terms of known paramagnetic defects alone. For example, in explaining the hydrogen annealing kinetics of electrically active in-

terface states it was assumed [17] that the different behavior of the (100) interface compared to (111) was a result of the presence of the P_{b1}^{100} center at the (100) interface. We now find that it is not P_{b1}^{100} but rather P_{b0}^{100} that behaves most differently, and that many interface states are not P_b centers at all.

The main lesson we may draw from this work is that the relevance of EPR studies on (111) interfaces in understanding the electrical and radiation response of the (100) interface is highly questionable. This is contrary to the conventional wisdom which holds that the results of fundamental studies of P_b^{111} can be largely carried over to the (100) interface, and that the existence of two defects at the (100) interface is a minor complication that affects the spectroscopy more than the physics. On the contrary, we now assert that P_{b0}^{100} is the dominant defect at the (100) interface, and that it is chemically not equivalent to P_b^{111}. Because the g tensors for P_{b0}^{100} and P_b^{111} are similar, it has long been thought that the two defects have a common structure, but the different chemical kinetics now points to significant structural differences. This might perhaps be reflected in the way nearby oxygen atoms are arranged which has so far only been measured in detail [10,11,24] for P_b^{111}. Likewise, many other characteristics of the Si/SiO_2 interface defects, such as their spatial distribution [13] and the relation to stress [19], which have been investigated in great detail on (111), may now require reinvestigation on (100) separately.

[1] D. L. Griscom, J. Electron. Mater. **21**, 762 (1992).
[2] Y. Nissan-Cohen and T. Gorczyca, IEEE Electron Dev. Lett. **9**, 287 (1988).
[3] D. J. DiMaria, E. Cartier, and D. Arnold, J. Appl. Phys. **73**, 3367 (1993).
[4] K. L. Brower and S. M. Meyers, Appl. Phys. Lett. **57**, 162 (1990).
[5] E. Cartier, J. H. Stathis, and D. Buchanan, Appl. Phys. Lett. **63**, 1510 (1993).
[6] E. H. Poindexter and P. J. Caplan, Prog. Surf. Sci. **14**, 210 (1983).
[7] K. L. Brower, Appl. Phys. Lett. **43**, 1111 (1983).
[8] A. H. Edwards, Phys. Rev. B **36**, 9638 (1987).
[9] M. Cook and C. T. White, Phys. Rev. B **38**, 9674 (1988).
[10] J. H. Stathis, S. Rigo, and I. Trimaille, Solid State Commun. **79**, 119 (1991).
[11] A. Stesmans and K. Vanheusden, Phys. Rev. B **44**, 11 353 (1991).
[12] K. L. Brower, Phys. Rev. B **33**, 4471 (1986).
[13] G. Van Gorp and A. Stesmans, Phys. Rev. B **45**, 4344 (1992).
[14] E. H. Poindexter, P. J. Caplan, B. E. Deal, and R. R. Razouk, J. Appl. Phys. **52**, 879 (1981).
[15] A. H. Edwards, in *The Physics and Chemistry of SiO_2 and the SiO_2 Interface,* edited by C. R. Helms and B. E. Deal (Plenum, New York, 1988), p. 271.
[16] J. H. Stathis and L. Dori, Appl. Phys. Lett. **58**, 1641 (1991).
[17] M. L. Reed and J. D. Plummer, J. Appl. Phys. **63**, 5776 (1988).
[18] Here we introduce the explicit indication of the interface orientation in naming the defects, in order to counteract the common but incorrect trend toward referring to the (111) defect as P_{b0}.
[19] A Stesmans, Phys. Rev. Lett. **70**, 1723 (1993).
[20] F. J. Feigl, R. Gale, H. Chew, C. W. Magee, and D.R. Young, Nucl. Instrum. Methods Phys. Res., Sect. B **1**, 348 (1984).
[21] Y. Y. Kim and P. M. Lenahan, J. Appl. Phys. **64**, 3551 (1988).
[22] J. T. Krick, P.M. Lenahan, and G. J. Dunn, Appl. Phys. Lett. **59**, 3437 (1991).
[23] J. H. Stathis and D. J. DiMaria, Appl. Phys. Lett. **61**, 2887 (1992).
[24] K. L. Brower, Z. Phys. Chem. Neue Folge **151**, 177 (1987).